Accurate adiabatic connection curve beyond the physical interaction strength

R. J. Magyar
Department of Physics, Rutgers University, New Jersey 08854-8019

W. Terilla
Department of Chemistry, Rutgers University, New Jersey 08854-8019

K. Burke
Department of Chemistry and Chemical Biology, Rutgers University, Piscataway, New Jersey 08854-8019

(Received 9 January 2003; accepted 11 April 2003)

In order to better approximate and understand the exchange-correlation functional in density functional theory, the adiabatic connection curve is accurately calculated beyond the physical interaction strength using a simulated scaling method. This is done for Hooke's atom, two interacting electrons in a harmonic well potential. Extrapolation of the accurate curve to the infinite-coupling limit agrees well with the strictly correlated electron hypothesis. The interaction strength interpolation is shown to be a good, but not perfect, fit to the adiabatic curve. Arguments about the locality of functionals and convexity of the adiabatic connection curve are examined in this regime. © *2003 American Institute of Physics.* [DOI: 10.1063/1.1579465]

I. INTRODUCTION

Density functional theory (DFT) is a popular computational method in solid-state physics and quantum chemistry since it is both simple and reliable.[1–3] Because of its wide range of applications and its ability to handle large systems, there is considerable interest in DFT and improving its accuracy. In DFT, the only part of the total energy to approximate is the exchange-correlation energy functional $E_{xc}[n]$. A formal and general expression for the exchange-correlation energy is according to the adiabatic connection[4]

$$E_{xc}[n]=\int_0^1 d\lambda\ U_{xc}[n](\lambda), \tag{1}$$

where $U_{xc}[n](\lambda)$ is the exchange-correlation potential energy of a density n at coupling constant λ [see Eq. (3)]. Analysis of the integrand $U_{xc}[n](\lambda)$ leads to many rigorous relationships that the exact exchange-correlation energy satisfies and approximate functionals should satisfy. For example, Görling and Levy obtained a perturbation series expression for the exchange-correlation energy[5] by expanding about the weak-interaction limit. Another fruitful result is the understanding of why hybrid functionals like PBE0 (Ref. 6) and B3LYP (Ref. 7) perform so well.[8–10]

Because the exchange-correlation energy is the area under the adiabatic connection curve between $\lambda=0$ and 1, most interest in $U_{xc}(\lambda)$ has been confirmed to this domain. However, there is no fundamental reason to restrict study to this domain. In fact, certain exact properties of the adiabatic connection curve outside this domain have been used to better approximate the curve between $\lambda=0$ and $\lambda=1$.[11] One example is consideration of the strong-interaction limit $\lambda\to\infty$. A model for this strongly interacting limit is the strictly correlated electron (SCE) hypothesis[11] which states that, because of the strong Coulomb repulsion, the individual electrons distribute themselves as far apart as possible, but are constrained to yield a given density. Finding one electron uniquely pins the others into position. Among other predictions, this SCE model says that U_{xc} can also be expanded about the strong-interaction strength limit ($\lambda\to\infty$). Information from this infinite limit combined with the Görling–Levy expansion about $\lambda=0$ leads to the suggestion of the interaction strength interpolation (ISI) for the entire curve. Exchange-correlation energies from the ISI are considerably more accurate than those using only the first two terms in the perturbation series.[12]

Another reason to consider large coupling strengths is that approximate exchange-correlation energy functionals for this limit might be more accurate.[13] It has long been known that standard approximate density functionals, such as the local density approximation (LDA) or the Perdew–Burke–Ernzerhof (PBE) generalized gradient approximation (GGA), are better for exchange and correlation together than they are for exchange alone. This is due to a cancellation of errors between approximations to the exchange and correlation energy.[10,14] If this cancellation between exchange and correlation grows with larger coupling constants, approximate density functionals in this regime will be more accurate.

The present work is a detailed study of some of these suggestions. We employ a simulated scaling procedure,[15] originally developed for the range $\lambda=0$–1, and extend the simulated adiabatic connection curve to larger coupling constants. At some point along the adiabatic connection curve, the simulating scale method is expected to break down. Nevertheless, the curve can be extrapolated from there to the infinite-coupling limit. This analysis yields interesting new information about the strong-interaction limit.

We work with Hooke's atom because it remains bound no matter how strongly the electrons interact. Hooke's atom is the unpolarized two electron system described by the Hamiltonian[16]

$$\hat{H} = -\frac{1}{2}(\nabla_1^2 + \nabla_2^2) + \frac{k}{2}(\mathbf{r}_1^2 + \mathbf{r}_2^2) + \frac{1}{|\mathbf{r}_1 - \mathbf{r}_2|}, \quad (2)$$

where k is the harmonic force constant, $\mathbf{r}_1$ and $\mathbf{r}_2$ are the position operators for each electron, and ∇_1^2 and ∇_2^2 are the Laplacian operators for each. Throughout, we use atomic units ($e^2 = \hbar = m_e = 1$) so that all energies are in hartrees and all lengths in Bohr radii. This is not just an exactly solvable model with Coulomb interactions, but also an important *physical system*. For example, many authors have used this system to model quantum dots.[17,18]

Although we could have performed calculations for the Hooke's atom at various harmonic well strengths, we will focus on $k = 1/4$. For this spring constant, Hooke's atom happens to admit an analytic solution.[19] Furthermore, for this k value, the correlation energy is comparable to that of the helium atom.

The simulated curves indicate that the SCE predictions for $U_{xc}(\infty)$ are correct. Next, assuming the validity of the SCE hypothesis, we generate a highly accurate simulation of the entire curve. This allows us to calculate higher derivatives of $U_{xc}(\lambda)$ around key points: $\lambda = 0$, 1, and ∞. This information should be useful for the testing and improvement of existing functionals. We also compare ISI with the accurate simulated result.

II. ADIABATIC CONNECTION THEORY

Three theoretical elements are vital to the content of this paper. These are the adiabatic connection curve, the strong-coupling limit, and the relationship between scale factor and coupling constant.

First, we review the adiabatic connection formalism. The integrand of Eq. (1) is

$$U_{xc}[n](\lambda) = \langle \Psi_n^{\min,\lambda} | \hat{V}_{ee} | \Psi_n^{\min,\lambda} \rangle - U[n], \quad (3)$$

where $U[n]$ is the Hartree energy, $\hat{V}_{ee}$ is the electron–electron Coulomb interaction, and $\Psi_n^{\min,\lambda}$ is the wave function that minimizes $\langle \Psi_n^{\min,\lambda} | \hat{T} + \lambda \hat{V}_{ee} | \Psi_n^{\min,\lambda} \rangle$ and yields the density $n(\mathbf{r})$. The functional, $U_{xc}[n](\lambda)$, as a function of λ, makes up the adiabatic connection curve. At $\lambda = 0$, Eq. (3) is just E_x, the exchange energy evaluated at a given density. Later, for convenience, we will subtract this contribution and write $U_c(\lambda) = U_{xc}(\lambda) - E_x$.

At small λ, one may write the Görling–Levy perturbation series[20,21]

$$U_{xc}[n](\lambda) = E_x[n] + 2E_c^{GL2}[n]\lambda + \mathcal{O}(\lambda^2), \quad \lambda \to 0, \quad (4)$$

where E_x is the exchange energy and $E_c^{GL2}[n]$ is the second-order contribution to the correlation energy. To get the exchange-correlation energy from Eq. (4), we need to integrate from $\lambda = 0$ to 1. Unfortunately, there is no guarantee that the higher-order terms will be negligible and that the series will converge.[12]

Other exact properties of U_{xc} might be useful to help understand this curve. An interesting limit is when $\lambda \to \infty$. This leads us to the second theoretical point, the strong-coupling limit. This limit corresponds to strongly interacting electrons which still yield the physical density. In this limit, the integrand is finite.[22] We can expand $U_{xc}(\lambda)$ about the infinite limit:

$$U_{xc}[n](\lambda) = U_{xc}[n](\infty) + U'_{xc}[n](\infty)/\sqrt{\lambda} + \mathcal{O}(1/\lambda), \quad \lambda \to \infty, \quad (5)$$

where $U_{xc}[n](\infty)$ and $U'_{xc}[n](\infty)$ are the zeroth and first terms in the expansion. It has been suggested that the electrons behave in a strictly correlated manner at this limit.[11] The electrons still produce a given density distribution, but finding one electron determines the position of all the others. Information about this limit can be incorporated into an interpolation formula which reproduces both limits exactly and can be integrated analytically. An example is the interaction strength interpolation.[12]

For spherically symmetric two-electron systems in three dimensions, the SCE model admits an exact solution for $U_{xc}(\infty)$ and provides one of two contributions to $U'_{xc}(\infty)$.[23] One question asked in this paper is how large the missing contribution to $U'_{xc}(\infty)$ is. We will calculate the SCE limit and part of the first correction term for Hooke's atom, $k = 1/4$, according to the expressions given by Seidl in Ref. 23.

The final point—the relationship between coupling constant and scale factor—is important for the procedure we used to simulate the adiabatic connection curve. A density $n(\mathbf{r})$ is scaled according to

$$n_\gamma(\mathbf{r}) = \gamma^3 n(\gamma \mathbf{r}), \quad 0 \leqslant \gamma < \infty, \quad (6)$$

with γ being the scale factor. The exchange-correlation energy at a coupling constant λ and density $n(\mathbf{r})$ is simply related to the exchange-correlation energy at a scaled density:[24,25]

$$E_{xc}^{\lambda}[n] = \lambda^2 E_{xc}[n_{1/\lambda}]. \quad (7)$$

The integrand in Eq. (1) is $U_{xc}(\lambda) = dE_{xc}^{\lambda}/d\lambda$. Under both coupling constant and scaling transformations, we can sometimes show how parts of the exact energy transform. For example,

$$E_x^{\lambda}[n] = \lambda E_x[n] \quad \text{or} \quad E_x[n_\gamma] = \gamma E_x[n]. \quad (8)$$

We use this observation later to identify scale factors between two scaled densities.

III. SIMULATED SCALING METHOD

In order to generate highly accurate adiabatic connection plots, we use the procedure developed by Frydel, Terilla, and Burke.[15] To find the adiabatic connection curve, we need $E_{xc}^{\lambda}[n]$ for a set of λ's. For Hooke's atom, we know the exact densities and the exact E_{xc} at different k values. Instead of changing λ, which is difficult, we use Eq. (7). A small change in the strength of external potential yields another density, qualitatively similar to the original density, but on a different scale. If we can solve the system exactly at this different external potential strength, we have an approximation to the exchange-correlation energy for a scaled density (see Fig. 1). When the densities that do not qualitatively change shape much, this scheme is highly accurate. To find $U_{xc}(\lambda)$, we differentiate Eq. (7) with this highly accurate

approximation to the exact $E_{xc}[n_{1/\lambda}]$. Including a first-order correction term increases the accuracy of this method:

$$E_c[n_\gamma] \approx E_c[n'] + \int d^3r\, v_c[n'](\mathbf{r})[n_\gamma(\mathbf{r}) - n'(\mathbf{r})] + \mathcal{O}(\delta n)^2, \tag{9}$$

where $v_c(\mathbf{r}) = \delta E_c[n]/\delta n(\mathbf{r})$ is the correlation contribution to the Kohn–Sham potential. This method gives highly accurate energies for Hooke's atom ($k=1/4$) and for helium when λ varies from 0 to 1. The error at $\lambda=0$ is 0.3 mhartree, and the estimated error for λ close to 1 less than 1 mhartree.[15]

For each simulated scaling, we must assign an appropriate scale factor, but which true scaled density does the approximately scaled density mimic? The original paper discusses several possibilities. They all require knowing how a chosen component of the energy changes with uniform density scaling. We use the E_x method:

$$\lambda = 1/\gamma = E_x[n]/E_x[n']. \tag{10}$$

See Table I for λ-k associations. Since we use E_x to assign λ, the $U_x(\infty)$ contribution to $U_{xc}(\infty)$ necessarily scales properly for all values of λ, and so we show only $U_c(\lambda)$.

In this paper, we examine the adiabatic connection curve at large interaction strengths. This method only works for $\lambda>1$ for systems that remain bound as the external potential is weakened. Even with this restriction, the method must ultimately fail as $\lambda\to\infty$. Specifically, for Hooke's atom, Cioslowski and Pernal showed that at a certain critical strength for the external potential, $k_c=0.0016$ ($\lambda_c=4.138$), the density changes shape qualitatively.[26] Beyond this value, the simulated scaling might no longer be a good approximation to exact scaling. On the other hand, the method fails for He almost immediately as the two-electron ion unbinds at nuclear charge, $Z=0.9$.

To test this procedure and to develop a rule for its reliability, we apply the procedure in a case where we already know the correct answer; namely, with an approximate functional. GGA mimics the complexity of the true functional better than, say, the local density approximation. Because of its first-principles derivation and reliability, we use the PBE approximation here.[27] Since we have the analytic form for the PBE functional, we can scale the input density to generate the entire adiabatic curve, Fig. 2. The curve is shown as a function of $\mu=1/\sqrt{\lambda}$ so that the region $\lambda\in 1,\infty$ can appear on a finite-sized plot.

TABLE I. Simulated scaling k and λ equivalences using the E_x scaling rule, Eq. (10), to determine λ.

k	λ	k	λ
1/4	1.000	1/4	1.000
1/16	1.460	1	0.689
1/64	2.151	4	0.478
1/256	3.197	16	0.334

PBE results for certain key λ values are listed in Table I. An explicit expression (13) for the PBE functional as $\mu\to 0$ is

$$U_{xc}^{\mathrm{PBE}}(\infty)[n] = \int d^3r\, n(r)\epsilon_x(n)\left(F_x^{\mathrm{PBE}}(s) + \frac{0.964}{1+y+y^2}\right), \tag{11}$$

where $y=0.2263s^2$, s is the reduced gradient, $\epsilon_x(n)$ is the exchange energy per particle of the uniform gas, and $F_x^{\mathrm{PBE}}(s)$ is an exchange enhancement factor.[27]

We need a criterion for how far along the adiabatic connection we can trust the simulated density scaling to mimic the exactly scaled density. Our criterion is to terminate the simulations at $\mu=\mu_c=1/\sqrt{\lambda_c}=0.4916$ where the density qualitatively changes shape.[26] Even at this point, the first-order correction in Eq. (9) still improves upon the zeroth-order simulation. This is a highly conservative estimate; it is likely that the curves are accurate to smaller μ's.

To get a prediction for $U_c(\mu=0)$, we must extrapolate the simulation to $\mu=0$. This is done by fitting the simulated data to an nth-order polynomial and extrapolating this polynomial to $\mu=0$. The third-order polynomial connecting four sample points best reproduces the known $U_c^{\mathrm{PBE}}(\infty)$. In Fig. 2, we show the exactly scaled PBE functional and the polynomial interpolation. We see that the simulated curve is almost on top of the exact curve. However, they do differ slightly in the $U_c(\mu=0)$ values. For the simulated curve, $U_c(\mu=0)=-0.357$, and the scaled result is -0.363 from Eq. (11), a 6-mhartree error.

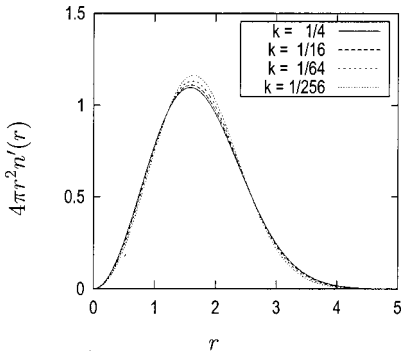

FIG. 1. Simulated scaling of the density. We start with Hooke's atom at $k=1/4$. Then, we solve at various other coupling constants and use simulated scaling to return us as closely as possible to the $k=1/4$ density.

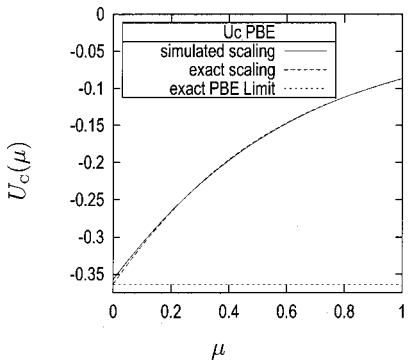

FIG. 2. PBE adiabatic connection curve for Hooke's atom ($k=1/4$): $U_C(\mu=1/\sqrt{\lambda})$. The solid line is generated using simulated scaling of the density and the dashed curve by exactly scaling the known functional. The exact PBE $U_C(\mu=0)$ limit is shown (short dashes).

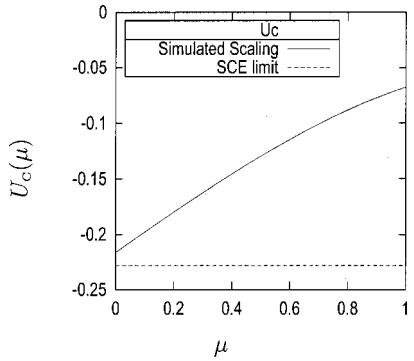

FIG. 3. Adiabatic connection curve for Hooke's atom ($k=1/4$): $U_C(\mu)$. The solid line is the simulated curve. The SCE limit is shown as a dashed line.

IV. EXTRAPOLATING TO THE INFINITE-INTERACTION-STRENGTH LIMIT

The simulated adiabatic connection curve for Hooke's atom $k=1/4$ in Fig. 3 approaches the SCE $U_c(\mu=0)$ limit. As in Sec. III for the PBE functional, we reproduce the entire curve by fitting the simulated points to a third-order polynomial. Since the simulated scaling method is only reliable between $\mu=1/2$ and 1, we must extrapolate the curve over the domain $\mu=0-1/2$ by a polynomial. The extrapolated prediction for $U_c(\mu=0)$, -0.206, is 22 mhartree from the strictly correlated electron prediction of -0.228. We do not expect as good agreement as in Sec. III because the true E_c functional is more complicated than a GGA, and we regard the result as consistent with the SCE hypothesis.

V. SIMULATING THE ENTIRE ADIABATIC CONNECTION CURVE

In Sec. IV, we used an extrapolation scheme to complete the adiabatic curve. Here, we combine the simulated part with the SCE electron limit to produce a highly accurate adiabatic connection curve for all coupling strengths. From this curve, we calculate the first terms in Taylor expansions about both $\lambda=0$, 1, and $\mu=0$, 1. Using these new results, we assess the accuracy of the ISI with accurate inputs.

The $\mu<1$ simulated adiabatic connection curve is shown in Fig. 4. The curve was generated by fitting the simulated

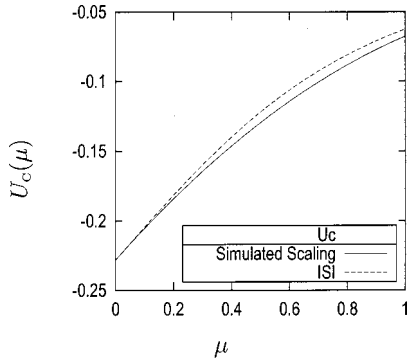

FIG. 4. Simulated adiabatic connection curve for Hooke's atom ($k=1/4$): $U_C(\mu)$. The solid line is the simulated curve with the SCE $U_C(\mu=0)$. The dashed curve is the ISI using exact inputs.

TABLE II. Higher derivatives of $U_C(\mu)$ with respect to μ for Hooke's atom ($k=1/4$).

μ	$U_C(\mu)$	$U_C'(\mu)$	$U_C''(\mu)$
0	−0.228	−0.235	−0.156
1	−0.068	0.088	0.221

data points from $\mu=0.5$ to 1 and including the SCE $U_c(\mu=0)$ in the point set. We used a third-order polynomial, the order that best reproduced the adiabatic curve for the PBE functional in Sec. III. This curve should be an excellent approximation to the exact curve. From the plot, we see that the derivative $dU_c(\mu)/d\mu$ is positive everywhere along the adiabatic curve. This implies that $dU_c(\lambda)/d\lambda$ is negative and the adiabatic curve is convex. All calculated $U_c(\lambda)$ curves for $0\leqslant\lambda\leqslant1$ have $dU_c(\lambda)/d\lambda<0$, but the inequality has never been gradually proved. Our result extends this observation to $\lambda\geqslant1$ for this system.

Derivatives of $U_c(\mu)$ are obtained from the coefficients in the polynomial extrapolation. Two higher derivatives of $U_c(\mu)$ with respect to μ are shown in Table II. Seidl's model for $U_c'(\mu=0)=0.281$ (Ref. 23) does not agree with the accurate $U_c'(\mu=0)$. This indicates that the missing contributions to the SCE $U_c'(\mu=0)$ mentioned by Seidl are, at least for this system, not negligible.

Several higher derivatives of $U_c(\lambda)$ with respect to λ are listed in Table III. Here, we need not restrict ourselves to a third-order polynomial interpolation because we have a dense sampling of data points over the range $\lambda=0-4$. The higher derivatives reported in terms of λ are expected to be highly accurate.

The ISI, as originally formulated,[12] is an interpolation scheme for the entire adiabatic connection curve. It used exact values of $\lambda=0$ and carefully chosen GGA values at $\mu=0$. We now ask how well the ISI with accurate inputs compares to the simulated curve. The answer tells us how good the choice of curve in the ISI is. For the inputs to the ISI, we use the exact E_x and E_c^{GL2}, which are derivable from the simulated curves in Ref. 15 and are given in Table IV. For $U_{xc}(\infty)$, we use the SCE prediction which, judging from the results in Sec. IV, we believe to be exact. For $U_c'(\mu=0)$, we input two different values: the accurate simulated value and Seidl's prediction. The results are shown in Table V. The ISI interpolation does not perform exceptionally well with accurate inputs as already noticed in Ref. 28. For example, the magnitude of $U_{xc}(1)$ is underestimated by 5 mhartree. This is perhaps a result of the way the $U_c'(\mu=0)$ limit is included in the interpolation equation. For this system, incorporating the accurate value for $U_c'(\mu=0)$ in the ISI does *not* greatly improve its accuracy.

TABLE III. Higher derivatives of $U_C(\lambda)$ with respect to λ for Hooke's atom ($k=1/4$).

λ	$U_C(\lambda)$	$U_C'(\lambda)$	$U_C''(\lambda)$	$U_C^{(3)}(\lambda)$	$U_C^{(4)}(\lambda)$
0	0.000	−0.101	0.095	−0.107	0.124
1	−0.0677	−0.044	0.032	−0.032	0.039

TABLE IV. Accurate results for Hooke's atom with $k=1/4$ evaluated on the exact densities.

	E_X	$2E_C^{GL2}$	E_C	$U_C(\mu=1)$	$U_C(\mu=0)$	$U_C'(\mu=0)$
PBE	−0.493	−0.168	−0.051	−0.087	−0.363	0.561
Exact	−0.515	−0.101	−0.039	−0.068	−0.228	0.235

In Fig. 5, we see how the PBE and LDA adiabatic connection curves compare to the accurate curve. The PBE curve clearly crosses the accurate curve. Because its exact limit $\lim_{\mu\to 0} U_{xc}^{LDA}(\mu)=1.964E_x^{LDA}$ is below the SCE prediction, the LDA curve must also cross the accurate one at some larger interaction strength. Since both curves cross the exact curve at some $\lambda>1$, the cancellation of errors between exchange and correlation in E_{xc}^{λ} will eventually grow smaller beyond some critical interaction strength and become an addition of errors. It has been argued that because the exchange correlation on-top hole grows more local as the interaction strength increases,[10,29] local functionals for E_{xc}^{λ} would work better as λ increases. This is certainly true for our system in the range $0\leqslant\lambda\leqslant 1$; however, the adiabatic plots indicate that as λ grows, the energy depends on the density in an increasing nonlocal way. The accuracy of the on-top hole is less relevant to the total energies in the strongly interacting region of the adiabatic connection curve. This is related to a self-correlation error as noted in Ref. 13. Both LDA and GGA functionals rely on the LDA treatment of the uniform gas, and the LDA cannot properly reproduce the Wigner crystallization limit due to this strong self-correlation error.[30] Meta-GGAs are self-correlation free and behave better in this limit.[31]

VI. CONCLUSION

In this work, we have extended the method of Ref. 15 to simulate the adiabatic connection curve to interaction strengths greater than the physical value for a simple model system. In doing so, we kept in mind that the method must fail at some μ_c as $\mu\to 0$ $(\mu=1/\sqrt{\lambda})$ and performed an extrapolation to the strong-interaction limit. This simulated curve agreed with the SCE hypothesis. To generate a highly accurate curve for $\mu=0$–1, we included the SCE $U_c(\mu=0)$ in the set of points and interpolated. Using this accurate adiabatic curve, we found higher derivatives at key coupling constants $\lambda=0$, 1, and ∞. Finally, we compared some popular approximate functionals to the accurate curve. These results will be useful in the formal analysis of the adiabatic connection curve, the testing of approximate functionals, and the construction of new functionals in DFT.

TABLE V. Interaction strength interpolation results for Hooke's atom with $k=1/4$. *Accurate* and *model* refer to the value of $U_c'(\mu=0)$. The accurate value is from our simulation and the model is from Seidl's model Ref. (23).

Method	$U_C'(\mu=0)$	$U_C(\lambda=1)$	Error	E_C	Error
ISI (accurate)	0.235	−0.063	8%	−0.036	6%
ISI (model)	0.281	−0.060	11%	−0.035	9%

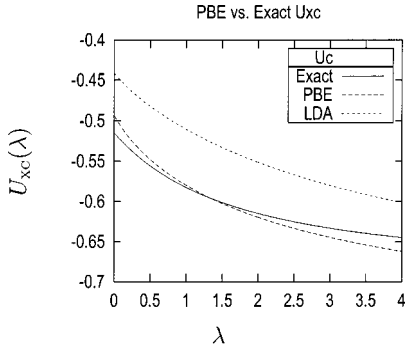

FIG. 5. Adiabatic connection curve for Hooke's atom using various functionals: The exact curve is the solid line, the PBE is the long-dashed line, and the local density approximation (LDA) is the short-dashed line.

ACKNOWLEDGMENTS

We would like to thank John Perdew for discussions and Takeyce Whittingham for computationally checking $U_{xc}^{PBE}(\infty)$. This work was supported by the National Science Foundation under Grant No. CHE-9875091.

[1] W. Kohn, Rev. Mod. Phys. **71**, 1253 (1999).
[2] P. Hohenberg and W. Kohn, Phys. Rev. **136**, B864 (1964).
[3] W. Kohn and L. J. Sham, Phys. Rev. **140**, A1133 (1965).
[4] D. C. Langreth and J. P. Perdew, Solid State Commun. **17**, 1425 (1975).
[5] A. Görling and M. Levy, Phys. Rev. A **50**, 196 (1994).
[6] C. Adamo and V. Barone, J. Chem. Phys. **110**, 6158 (1999).
[7] A. D. Becke, J. Chem. Phys. **98**, 5648 (1993).
[8] K. Burke, J. P. Perdew, and M. Ernzerhof, in *Electronic Density Functional Theory: Recent Progress and New Directions*, edited by J. F. Dobson, G. Vignale, and M. P. Das (Plenum, New York, 1997), p. 57.
[9] J. P. Perdew, M. Ernzerhof, and K. Burke, J. Chem. Phys. **105**, 9982 (1996).
[10] K. Burke, M. Ernzerhof, and J. P. Perdew, Chem. Phys. Lett. **265**, 115 (1997).
[11] M. Seidl, J. Perdew, and M. Levy, Phys. Rev. A **59**, 51 (1999).
[12] M. Seidl, J. Perdew, and S. Kurth, Phys. Rev. Lett. **84**, 5070 (2000).
[13] M. Seidl, J. Perdew, and S. Kurth, Phys. Rev. A **62**, 012502 (2000).
[14] K. Burke, J. P. Perdew, and M. Levy, Phys. Rev. A **53**, R2915 (1996).
[15] D. Frydel, W. Terilla, and K. Burke, J. Chem. Phys. **112**, 5292 (2000).
[16] S. Kais, D. R. Herschbach, N. C. Handy, C. W. Murray, and G. J. Laming, J. Chem. Phys. **99**, 417 (1993).
[17] U. Merkt, J. Huser, and M. Wagner, Phys. Rev. B **43**, 7320 (1991).
[18] R. M. G. Garca-Casteln, W. S. Choe, and Y. C. Lee, Phys. Rev. B **57**, 9792 (1998).
[19] M. Taut, Phys. Rev. A **48**, 3561 (1993).
[20] A. Görling and M. Levy, Phys. Rev. B **47**, 13 105 (1993).
[21] A. Görling and M. Levy, Int. J. Quantum Chem. **29**, 93 (1995).
[22] M. Levy, Phys. Rev. A **43**, 4637 (1991).
[23] M. Seidl, Phys. Rev. A **60**, 4387 (1999).
[24] K. Burke, in *Electronic Density Functional Theory: Recent Progress and New Directions*, edited by J. F. Dobson, G. Vignale, and M. P. Das (Plenum, New York, 1997), p. 19.
[25] M. Levy and J. P. Perdew, Phys. Rev. A **32**, 2010 (1985).
[26] J. Cioslowski and K. Pernal, J. Chem. Phys. **113**, 8434 (2000).
[27] J. P. Perdew, K. Burke, and M. Ernzerhof, Phys. Rev. Lett. **77**, 3865 (1996); **78**, 1396(E) (1997).
[28] J. Perdew, S. Kurth, and M. Seidl, Int. J. Mod. Phys. B **15**, 1672 (2001).
[29] K. Burke, J. Perdew, and M. Ernzerhof, J. Chem. Phys. **109**, 3760 (1998).
[30] H. B. Shore, E. Zaremba, J. H. Rose, and L. Sanders, Phys. Rev. B **18**, 6506 (1978).
[31] J. P. Perdew, S. Kurth, A. Zupan, and P. Blaha, Phys. Rev. Lett. **82**, 2544 (1999); **82**, 5179(E) (1999).